AJNR

Cerebral Ischemia Detected with Diffusion-Weighted MR Imaging after Stent Implantation in the Carotid Artery

Horst J. Jaeger, Klaus D. Mathias, Elke Hauth, Robert Drescher, H. Martin Gissler, Svenja Hennigs and Andreas Christmann

Cerebral Ischemia Detected with Diffusion-Weighted MR Imaging after Stent Implantation in the Carotid Artery

Horst J. Jaeger, Klaus D. Mathias, Elke Hauth, Robert Drescher, H. Martin Gissler, Svenja Hennigs, and Andreas Christmann

BACKGROUND AND PURPOSE: Concern regarding the safety of stent implantation in the carotid artery exists because of the risk of cerebral embolization during the procedure. The purpose of this prospective study was to determine the incidence of new areas of cerebral ischemia, as detected by using diffusion-weighted MR imaging after stent implantation in the carotid artery.

METHODS: Diffusion-weighted MR imaging of the brain was performed in 67 patients with 70 high-grade stenoses of the carotid artery before and 24 hours after stent implantation.

RESULTS: The neurologic status of the patients was unchanged after 69 of 70 procedures. During one procedure, symptomatic cerebral embolization occurred. Diffusion-weighted MR images showed new ipsilateral lesions after stent implantation in 20 patients (29%), including the symptomatic patient, and new contralateral lesions in six patients (9%). Fifty-two of 59 postprocedural lesions occurred in the vascular territory supplied by the treated vessel. The occurrence of new postprocedural ipsilateral lesions was not significantly correlated with patient demographic data, characteristics of the stenoses, or details of the procedure.

CONCLUSION: In 29% of the procedures, stent implantation in the carotid artery was associated with new areas of cerebral ischemia, as detected by using diffusion-weighted MR images; these findings indicated the occurrence of cerebral microemboli during such procedures. In all patients except one, the new lesions were clinically silent.

The purpose of treating a stenosis of the carotid artery is to prevent stroke. In recent years, stent implantation has been developed as an alternative to surgical treatment for high-grade stenoses in the carotid artery (1–5). In a survey of 36 major interventional centers worldwide that regularly perform stent implantation in the carotid artery, the combined periprocedural stroke and death rate in 5210 procedures was 5.07% (5). The distal embolization of plaque material during the procedure is considered the cause of most neurologic complications after stent implantation in the carotid artery (1–8).

At present, diffusion-weighted MR imaging of the brain is the most sensitive tool for the detection of cerebral ischemia (9–15). It has been used to detect structural damage of the brain due to cerebral embolism after cerebral angiography, neurointerventional procedures, and carotid endarterectomy (16–19).

The purpose of this prospective study was to determine the incidence of new areas of cerebral ischemia, as detected by using diffusion-weighted MR imaging after stent implantation in the carotid artery.

Methods

Patient Population

Our institutional review board approved this prospective study. Informed consent was obtained from each patient after the nature of the procedure had been fully explained. Ninety-one patients underwent 94 stent implantation procedures in the carotid artery to treat high-grade stenoses during a 12-month period. The inclusion criteria for carotid artery stent placement were a symptomatic stenosis of the carotid artery of more than 70% or an asymptomatic stenosis of more than 80%. The exclusion criterion was either an inability to gain access to the appropriate common carotid artery (CCA) or an inability to cross the stenosis of the carotid artery with the guidewire or a low-profile percutaneous transluminal coronary angioplasty (PTCA) balloon. Patients were eligible for inclusion in this prospective study if they had no contraindications for MR examination. Diffusion-weighted MR imaging of the brain was performed in 67 patients before and 24 hours after 70 proce-

TABLE 1: Patient characteristics

| | Patients | | | |
Characteristics	All (n = 67)	With Positive DW Findings (n = 47)	With Negative DW Findings (n = 20)	P Value*
Demographic				
Sex				.382
Male	47 (70)	31 (66)	16 (80)	NA
Female	20 (30)	16 (34)	4 (20)	NA
Age (y)†	67 ± 9.1 (44–86)	66 ± 9.3 (44–86)	70 ± 7.8 (57–86)	.076
Medical history				
Hypertension	57 (85)	39 (83)	18 (90)	.711
Coronary artery disease	45 (67)	30 (64)	15 (75)	.412
Peripheral vascular disease	35 (52)	26 (55)	9 (45)	.594
Diabetes mellitus	28 (42)	21 (45)	7 (35)	.591
Hypocholesterolemia	53 (79)	39 (83)	14 (70)	.325
Cardiac arrhythmia	20 (30)	14 (30)	6 (30)	>.99
T2-weighted MR imaging				
Cerebral atrophy	46 (69)	31 (66)	15 (75)	.571
Subcortical arteriosclerotic encephalopathy	58 (87)	41 (87)	17 (85)	>.99
Cerebral infarction				
Ipsilateral	13 (19)	8 (17)	5 (25)	.507
Contralateral	9 (13)	7 (15)	2 (10)	.714

Note.—Data in parentheses are percentages, unless otherwise specified.

* NA indicates not applicable.

† Data are the mean ± SD. Data in parentheses are the range.

dures. In the remaining 24 patients, MR imaging could not be performed because of the presence of an intracranial aneurysmal clip (two patients), a pacemaker (eight patients), or claustrophobia (14 patients).

All patients underwent neurologic examination before and 24 hours after the procedure. Clinical and Doppler sonographic follow-up was performed 30 days after the procedure. The demographic data and pertinent features of the medical history of the patients were recorded. (Tables 1 and 2)

Technique of the Intervention

Two experienced operators (H.J.J., K.D.M.) performed all of the procedures. Each had performed several hundred stent placement procedures in the carotid artery before the start of the study. The day before the procedure, the patients received 500 mg of acetylsalicylic acid (ASA) and 300 mg of clopidogrel. The administration of 100 mg of ASA once daily was continued as a permanent medication, and 75 mg of clopidogrel was given once daily for 3 months. All procedures were performed with local anesthesia administered via percutaneous transfemoral or transbrachial access. During the procedure, the patients received 5000–10,000 IU of heparin intraarterially to attain an activated clotting time (ACT) of more than 200 seconds. The procedure was started with an aortic arch injection to detect atherosclerotic disease at the origin of the supraaortic vessels and to obtain anatomic information to guide selective catheterization. This step was followed by selective angiography of both CCAs and at least one subclavian or vertebral artery. The grade of the stenosis was measured according to the North American Symptomatic Carotid Endarterectomy Trial method (20) (Table 2).

Two procedural techniques were used for stent placement: the over-the-wire (OTW) technique and the long-sheath method.

In the OTW technique, the stenosis was visualized through the diagnostic catheter with the road map or overlay technique. A 300-cm-long 0.020-inch guidewire (Steerable guidewire with 6-cm flexible J curved tip; Boston Scientific Vascular, Natick, MA) then was passed through the stenosis. The tip of the wire was placed in the distal internal carotid artery (ICA) at the base of skull. The predilation procedure, stent placement, and post-

dilation procedure were performed over this wire. A Tuohy-Borst adapter was used for angiographic control. In the OTW technique, no guiding catheter or long sheath is used to gain access to the CCA.

In the long-sheath method, a 300-cm-long 0.035-inch guidewire (Amplatz Super Stiff guidewire with 6-cm flexible straight tip; Boston Scientific Vascular) was placed in the external carotid artery, and a 7F 90-cm-long sheath (Super Arrow Flex sheath; Arrow, Reading, PA) was advanced in the CCA. The sheath was irrigated with pressurized isotonic sodium chloride solution with heparin. Through the sidearm of the sheath, the stenosis was visualized with the road map or overlay technique. A 300-cm-long 0.014-inch guidewire (Choice Extra Support; Boston Scientific Vascular) then was passed through the stenosis. The sidearm of the sheath was used for angiographic control. In this method, the long sheath serves as the guiding catheter.

Predilation was performed with a 4-mm low-profile PTCA balloon (Bijou; Boston Scientific Vascular). A self-expandable stent (Wallstent; Boston Scientific Vascular) was placed in the ICA, CCA, or both, depending on the location of the stenosis. Postdilation was performed with a 5-mm percutaneous transluminal angioplasty balloon (Smash; Boston Scientific Vascular). Immediately before pre- and postdilation, 0.5 mg of atropine was given intravenously to counteract reflex bradycardia due to pressure on the baroreceptors at the carotid bifurcation. Finally, angiograms of the stent and the intracranial circulation of the treated carotid artery were obtained. No cerebral protection devices were used.

One hour after the procedure, the arterial sheath was removed if the patient had an ACT of less than 140 seconds and if his or her neurologic and hemodynamic conditions were stable (Table 3).

Technique of MR Imaging

MR imaging was performed by using a 1.5-T whole-body system (Vision; Siemens Medical Systems, Iselin, NJ) with a dedicated head coil. The MR studies included axial T2-weighted and diffusion-weighted sequences. The T2-weighted sequence was a fast spin-echo sequence with the following

TABLE 2: Characteristics of the stenoses

Characteristic	All (n = 70)	With Positive DW Findings (n = 50)	With Negative DW Findings (n = 20)	P Value*
Symptoms				
Present	52 (75)	38 (76)	14 (70)	.763
Present in the last 3 mo	42 (60)	30 (60)	12 (60)	>.99
Absent	18 (25)	12 (24)	6 (30)	.763
Cause				.408
Atherosclerotic	63 (90)	45 (90)	18 (90)	NA
Surgery	6 (9)	5 (10)	1 (5)	NA
Irradiation	1 (1)	0 (0)	1 (5)	NA
Side				.285
Right	40 (57)	31 (62)	9 (45)	NA
Left	30 (43)	19 (38)	11 (55)	NA
Grade (%)†	84 ± 7.9 (60–98)	83 ± 7.3 (60–98)	86 ± 9.3 (62–98)	.131
Classification				.493
0–29%	0 (0)	0 (0)	0 (0)	NA
30–69%	2 (3)	1 (2)	1 (5)	NA
70–99%	68 (97)	49 (98)	19 (95)	NA
Location				.182
ICA at bifurcation	35 (50)	24 (48)	11 (55)	NA
Proximal ICA	32 (46)	25 (50)	7 (35)	NA
CCA	3 (4)	1 (2)	2 (10)	NA
Length				.259
<1 cm	47 (67)	36 (72)	11 (55)	NA
>1 cm	23 (33)	14 (28)	9 (45)	NA
Morphology				.796
Eccentric	37 (53)	27 (54)	10 (50)	NA
Concentric	33 (47)	23 (46)	10 (50)	NA
Ulcerations	17 (24)	14 (28)	3 (15)	.359
Contralateral ICA occlusion	6 (9)	5 (10)	1 (5)	.666

Note.—Data in parentheses are percentages, unless otherwise specified.

* NA indicates not applicable.

† Data are the mean ± SD. Data in parentheses are the range.

parameters: single echo; 5700/119/1 [TR/TE/excitations]; echo train length, 15; matrix, 240 × 512; field of view (FOV), 201 × 230 mm; section thickness, 5 mm; intersection gap, 1.5 mm; and total acquisition time, 1.36 minutes. The diffusion-weighted sequence was a spin-echo echo-planar sequence with the following parameters: 6000/103/1; FOV, 230 × 230 mm; matrix, 96 × 200; section thickness, 5 mm; intersection gap, 1.5 mm; total acquisition time, 0.30 min; and fat saturation. The diffusion-weighted sequence was performed with two levels of diffusion sensitization: b = 0 and b = 1000 s/mm². The higher level of diffusion sensitization was replicated in each of the three principal gradient directions (x, y, and z planes). The diffusion-weighted images from each of three diffusion-sensitized acquisitions were separately displayed for analysis.

MR examinations were performed before and 24 hours after the procedures. On the T2-weighted images, the presence of cerebral atrophy, subcortical arteriosclerotic encephalopathy, and cerebral infarction was determined. On the diffusion-weighted images, the presence of signal intensity abnormalities was recorded. With all abnormalities on diffusion-weighted images, the size, location, and vascular distribution were determined. All abnormalities on diffusion-weighted images were correlated with the findings on the T2-weighted images. The results of the pre- and postprocedural MR examinations were compared. Two neuroradiologists (H.J.J., H.M.G.) who were unaware of the clinical status of the patients evaluated all of the MR images. In cases of disagreement, a third neuroradiologist (K.D.M.) reviewed the images, and a decision was made by consensus.

Definitions

The upper area of the brain was defined as the part of the brain above the lateral ventricles, the middle area was defined as the part between the lateral ventricles and the third ventricle, and the lower area was defined as the part below the third ventricle. The cortical and subcortical areas were defined as the cortical and subcortical parts of the cerebrum, respectively, and the deep area was defined as the basal ganglia and thalamus. Ipsilateral was defined as the side of the treated carotid artery. Contralateral was defined as the side opposite that of the treated carotid artery. The part of the occipital lobes, basal ganglia, and thalamus supplied by the vertebrobasilar vascular axis were included in the definition of the contralateral side. New lesions were defined as lesions that were present only on the postprocedural MR images. Procedures or patients with negative diffusion-weighted imaging results were those without new ipsilateral lesions after the intervention. Procedures or patients with positive diffusion-weighted imaging results were those with new ipsilateral lesions after the intervention.

Statistical Analysis

The Fisher exact and Freeman-Halton tests were used to analyze significant differences between the group with positive diffusion-weighted imaging results and that with negative diffusion-weighted imaging results if the considered variable was nominal (21). The Wilcoxon rank sum test was used to analyze significant differences between the groups if the considered variable was continuous (22). All tests were computed with a

TABLE 3: Details of procedures

| Detail | Procedures | | | |
	All (n = 70)	With Positive DW Findings (n = 50)	With Negative DW Findings (n = 20)	P Value*
Access				.194
Transfemoral	67 (96)	49 (98)	18 (90)	NA
Transbrachial	3 (4)	1 (2)	2 (10)	NA
Technique				.107
OTW	61 (87)	46 (92)	15 (75)	NA
Long sheath	9 (13)	4 (8)	5 (25)	NA
Predilation	65 (93)	47 (94)	18 (90)	.619
Type of Wallstent				.551
Rolling membrane	10 (14)	6 (12)	4 (20)	NA
Easy	44 (63)	33 (66)	11 (55)	NA
OTW	16 (23)	11 (22)	5 (25)	NA
Location of stent				.122
ICA	9 (13)	6 (12)	3 (15)	NA
ICA and/or CCA	59 (84)	44 (88)	15 (75)	NA
CCA	2 (3)	0 (0)	2 (10)	NA
Postdilation	61 (87)	44 (88)	17 (85)	.708
Grade of remaining stenosis (%)†	5.8 ± 7.7 (0–29)	5.5 ± 6.8 (0–29)	6.6 ± 9.8 (0–29)	.889

Note.—Data in parentheses are percentages, unless otherwise specified.

* NA indicates not applicable.

† Data are the mean ± SD. Data in parentheses are the range.

5% level of significance. The computations were performed with the statistical software packages SAS and StatXact for Windows.

Results

Results of the Procedure and Complications

All 70 stent implantations in the carotid artery were successful (Table 3). During 69 procedures, the neurologic status of the patient was unchanged. During one procedure, symptomatic ipsilateral embolization, with occlusion of the M1 segment of the middle cerebral artery (MCA), occurred. Local intraarterial thrombolysis of the MCA was performed with 40 mg of recombinant tissue plasminogen activator. After thrombolysis, the M1 segment of the MCA was reopened. During another procedure, asymptomatic embolization occurred. The angiogram of the intracranial circulation obtained after the procedure demonstrated an nonocclusive embolus in a branch of the MCA. Urokinase (100,000 IU) was administered into the ICA. A control angiogram obtained after the infusion showed that the embolus had dissolved.

The 30-day clinical follow-up disclosed no new neurologic symptoms or deficits. The patient in whom symptomatic ipsilateral embolization occurred had residual paresis of the contralateral hand and arm. All stents were patent, as shown on Doppler sonograms.

Results of MR Imaging

Results of the T2-weighted MR imaging are shown in Table 1. Before the procedure, diffusion-weighted MR images revealed ipsilateral cerebral lesions in 10 (14%) of 70 cases. The total number of preprocedural ipsilateral lesions was 24. In one of the cases with ipsi-

lateral preprocedural lesions, a contralateral lesion also was present. In three of these 10 procedures, new lesions occurred after stent implantation (Table 4).

After the procedure, new ipsilateral lesions were seen in 20 (29%) of 70 cases, and new contralateral lesions in were seen six (9%). The average number of postprocedural ipsilateral lesions was 2.6 (range, 1–6) and of contralateral lesions 1.2 (range, 1–2). In four of the six cases with contralateral lesions, new ipsilateral lesions also occurred (Table 4, Figs 1–3).

Fifty-two (88%) of 59 postprocedural lesions occurred on the ipsilateral side. Forty-four (75%) postprocedural lesions had a diameter of less than 5 mm. Fifty-four (92%) of the postprocedural lesions were in the upper and middle areas of the brain. Fifty-six (95%) postprocedural lesions occurred in the cortical and subcortical areas of the brain. Forty-seven (80%) postprocedural lesions were in the frontal and parietal lobes. Fifty-two (88%) postprocedural lesions occurred in the cortical distribution of the anterior cerebral artery (ACA) and MCA. The contralateral lesions included two lesions that occurred in areas of the brain supplied by the vertebrobasilar axis: one in the basal ganglia and one in the occipital lobe (Table 4).

The diffusion-weighted images in the patient in whom symptomatic embolization occurred showed four new postinterventional lesions: two with diameters of less than 5 mm and two lesions with diameters of 15 and 40 mm. This patient had also three ipsilateral preinterventional lesions. The patient with the asymptomatic embolus had three ipsilateral postinterventional lesions: two with diameters of less than 5 mm and one with a diameter of 5–10 mm on diffusion-weighted images (Fig 4).

The statistical analysis between the group with positive diffusion-weighted imaging results and that with

TABLE 4: Lesion characteristics on DW MR images of the brain

	Lesion			
Characteristic	Ipsilateral Preprocedural	Contralateral Postprocedural	Ipsilateral	Contralateral
Procedures with lesions*	10 (14 [7, 25])	1 (1 [0, 7])	20 (29 [19, 41])	6 (9 [4, 17])
No. of lesions				
Total	24	1	52	7
Average	2.4	NA	2.6	1.2
Range	1–6	NA	1–8	1–2
Size				
<5 mm	10 (42)	0 (0)	36 (69)	6 (86)
5–10 mm	7 (29)	0 (0)	11 (21)	0 (0)
>10 mm	7 (29)	1 (100)	5 (10)	1 (14)
Location				
Vertical distribution				
Upper area of brain	15 (63)	1 (100)	27 (52)	4 (57)
Middle area of brain	9 (38)	0 (0)	20 (39)	3 (43)
Lower area of brain	0 (0)	0 (0)	5 (10)	0 (0)
Horizontal distribution				
Cortical or subcortical area	24 (1000)	1 (100)	50 (96)	6 (86)
Deep area	0 (0)	0 (0)	2 (4)	1 (14)
Cerebral distribution				
Frontal lobe	0 (0)	0 (0)	4 (8)	3 (43)
Parietal lobe	23 (96)	1 (100)	38 (73)	2 (29)
Temporal lobe	1 (4)	0 (0)	5 (10)	0 (0)
Occipital lobe	0 (0)	0 (0)	3 (6)	1 (14)
Basal ganglia	0 (0)	0 (0)	1 (2)	0 (0)
Thalamus	0 (0)	0 (0)	1 (2)	1 (14)
Vascular distribution†				
ACA cortical branches	1 (4)	1 (100)	5 (10)	2 (29)
ACA deep branches	0 (0)	0 (0)	1 (2)	0 (0)
MCA cortical branches	23 (96)	0 (0)	42 (82)	3 (43)
MCA deep branches	0 (0)	0 (0)	0 (0)	0 (0)
PCA cortical branches	0 (0)	0 (0)	3 (6)	1 (14)
PCA deep branches	0 (0)	0 (0)	1 (2)	1 (14)

Note.—Total of procedures was 70. Data in parentheses are percentages, unless otherwise specified. NA indicates not applicable.

* Data in brackets are the 95% confidence intervals.

† PCA indicates posterior cerebral artery.

FIG 1. Images obtained in a 70-year-old man with an asymptomatic stenosis of the carotid artery.

A, Right anterior oblique angiogram shows a 94% stenosis of the right ICA.

B, Right anterior oblique angiogram shows the result after stent implantation.

C, Postprocedural axial diffusion-weighted MR image (6000/103/1) shows a new ipsilateral lesion (<5 mm) in the cortical territory of the MCA (*arrow*).
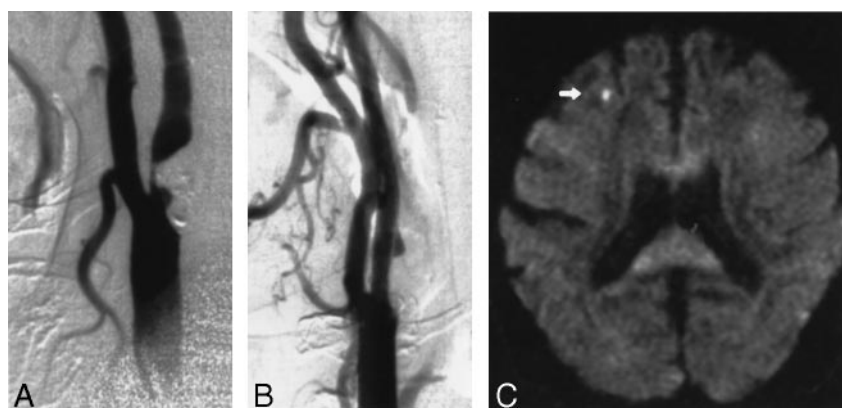
negative diffusion-weighted imaging results did not reveal any significant difference in patient demographic data, characteristics of the stenoses, or details of the procedures (Tables 1–3).

Of all postprocedural lesions seen on DW images, 17 (29%) of 59 also were visible on T2-weighted MR images. Their visibility on the T2-weighted images was size dependent. Lesions that were smaller than 5 mm on diffusion-weighted images were visible on T2-weighted MR images in 17% of the cases; those

5–10 mm, in 36% of the cases; and those larger than 10 mm, in 100% of the cases (Fig 3).

Discussion

Jordan et al (6) determined the rate of embolus detection with transcranial Doppler sonography during stent implantation in the carotid bifurcation; the mean was 74.0 emboli per procedure. In only three of 40 procedures were no emboli detected. In an ex vivo
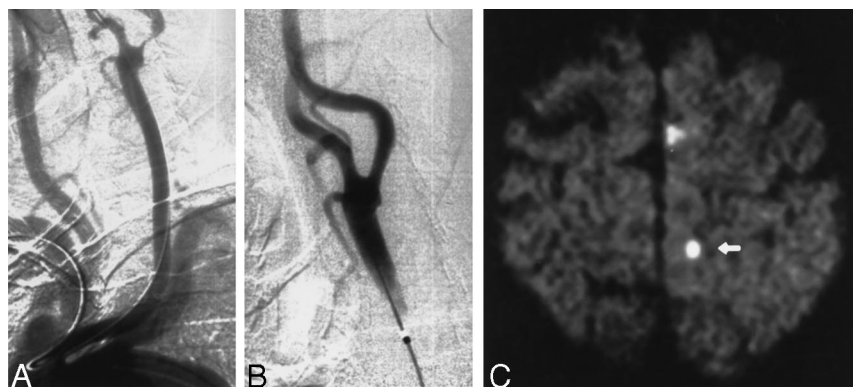
Fig 2.   Images obtained in a 86-year-old man with a symptomatic stenosis of the carotid artery.

A, Left anterior oblique angiogram (transbrachial approach) shows an 87% stenosis of the left ICA.

B, Left anterior oblique angiogram shows the result after stent implantation.

C, Postprocedural axial diffusion-weighted MR image (6000/103/1) shows six new ipsilateral lesions (5–10 mm) in the cortical territory of the ACA (*arrow*).
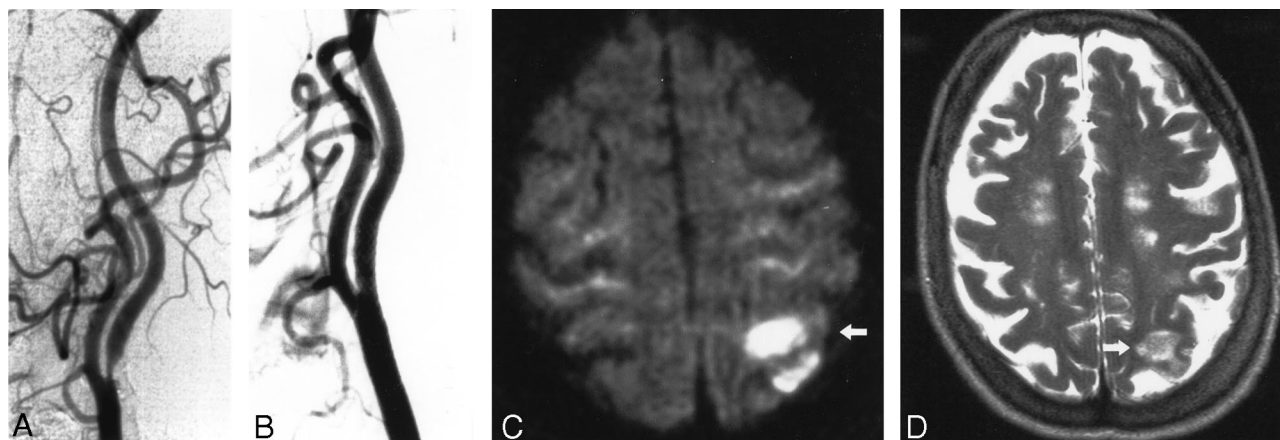

Fig 3.   Images obtained in a 73-year-old woman with a symptomatic stenosis of the carotid artery.

A, Left anterior oblique angiogram shows an 85% stenosis of the left ICA.

B, Left anterior oblique angiogram shows the result after stent implantation.

C, Postprocedural axial diffusion-weighted MR image (6000/103/1) shows eight new ipsilateral lesions (15–20 mm) in the cortical territory of the MCA (*arrow*).

D, Postprocedural axial T2-weighted MR image (5700/119/1) obtained at a corresponding level shows a new area of hyperintensity (*arrow*) that was not present in *C*.
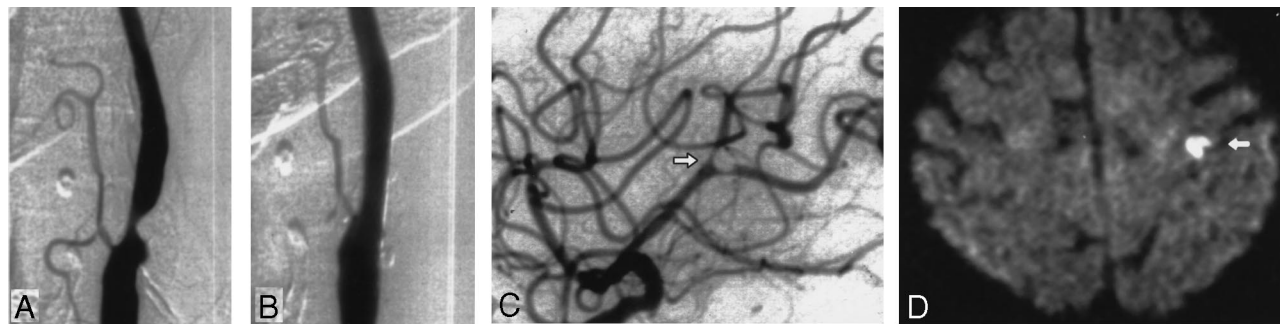

Fig 4.   Images obtained in a 76-year-old woman with a symptomatic stenosis of the carotid artery.

A, Left anterior oblique angiogram shows a 79% stenosis of the left ICA.

B, Left anterior oblique angiogram shows the result after stent implantation.

C, Lateral angiogram shows the intracranial circulation of the treated side after a procedure with a nonocclusive embolus in a branch of the MCA (*arrow*). The patient was symptomatic during the whole procedure. An angiogram of the intracranial circulation obtained after the infusion of 100,000 IU of urokinase into the ICA demonstrated complete disappearance of the embolus (not shown).

D, Postprocedural axial diffusion-weighted MR image (6000/103/1) shows eight new ipsilateral lesions (5–10 mm) in the cortical territory of the MCA (*arrow*).

model of the carotid bifurcation, Ohki et al (7) observed distal embolization during stent implantation in the carotid bifurcation in all cases. They observed a median of 15 emboli, with a range of two to 126, per procedure. Manninen et al (8) demonstrated that embolization occurred during all stent implantation proce- dures involving the distal carotid bifurcation in cadavers in situ. These results from transcranial Doppler moni- toring and experimental studies show that embolization may occur in nearly all stent implantation procedures in the carotid artery.

Postprocedural diffusion-weighted MR images in

20 (29%) of the 70 cases showed new ipsilateral lesions. Fifty-two (88%) of the 59 postinterventional lesions occurred in the vascular territory supplied by the treated carotid artery. This result indicates that the most likely causes of these signal intensity abnormalities are emboli that are released during the procedure and delivered into the distal circulation of the treated vessel. We observed that most lesions were smaller than 5 mm and occurred in the distribution of the cortical branches of the MCA and ACA, in the parietal and frontal lobes, and in the upper and middle areas of the brain. This type and distribution of the lesions can be considered the embolic pattern of cerebral embolization. This finding can be explained by the fact that particles released during the procedure travel a straight path with the blood flow to the cortical branches of the MCA and ACA.

Postprocedural diffusion-weighted MR images in six (9%) of 70 cases showed new contralateral postprocedural lesions. These lesions also had the embolic pattern, but far fewer contralateral lesions were present than were ipsilateral lesions. All of our patients received an aortic arch injection and underwent three- or four-vessel cerebral angiography before the procedure. This result indicates that guidewire or catheter manipulation during a diagnostic study can cause lesions, as depicted on the diffusion-weighted MR images herein. Bendszus et al (16) found new lesions on the diffusion-weighted brain MR images in 17 (29%) of 59 patients after diagnostic cerebral angiography. The lower incidence of contralateral lesions in our patients may be explained by the fact that we administered systemic heparin in all of our patients at the beginning of the procedure (23).

Van Everdingen et al (14) demonstrated that diffusion-weighted MR images depicted 44 (98%) of 45 ischemic lesions, in contrast with results of fluid-attenuated inversion recovery, proton density–weighted, and T2-weighted imaging, which showed only 91%, 80%, and 71% of all lesions, respectively. In our series, only 17 (28%) of 61 lesions were visible on the T-weighted images. Compared with larger lesions, smaller lesions were less likely to be seen on the T2-weighted images. This finding underscores that the number of cerebral lesions revealed by diffusion-weighted MR imaging cannot be compared with that of other MR examinations and that diffusion-weighted MR imaging should be considered the criterion standard in the detection of cerebral lesions after stent implantation in the carotid artery.

What the signal intensity changes on the diffusion-weighted MR images represent is not yet completely understood. Kidwell et al (13) demonstrated that five of nine patients with transient ischemic attacks who had early abnormalities on diffusion-weighted images did not have evidence of established infarction on follow-up images. Van Everdingen et al (14) showed that all 44 hyperintense lesions on diffusion-weighted images in patients with acute stroke evolved into infarcts that were disclosed on follow-up images. In humans, once a cell demonstrates increased signal intensity on diffusion-weighted images, the time frame for restoration of the oxygen and metabolite supply and for reversal may be very short. Beauchamp et al (10) hypothesized that high-signal-intensity lesions on diffusion-weighted MR images indicate infarction when findings on T2-weighted images are positive. Therefore, a signal intensity abnormality on diffusion-weighted MR images obtained 24 hours after the event should be considered an early marker of infarction, especially if high signal intensity is shown on T2-weighted images.

At present, it cannot be completely determined which step of the stent placement procedure causes most of these lesions. Manninen et al (8) demonstrated that embolization occurred both during stent placement and the postdilation procedure in the distal carotid artery in cadavers in situ. Emboli can occur during diagnostic angiography before the intervention (16–17). They also may occur during the initial crossing of the stenosis with the guidewire or during balloon angioplasty, stent placement, or postdilation of the stent (6–8). Further investigations with transcranial Doppler monitoring during stent implantation in the carotid artery are necessary to identify the steps of the procedure that are most likely to be responsible for distal embolization.

Some controversy about the clinical importance of cerebral microemboli exists. In our series, only one of the 20 patients with new ipsilateral postprocedural lesions, as depicted on diffusion-weighted images, was clinically symptomatic. All six patients with new contralateral lesions were asymptomatic. In the study by Lövblad et al (18), four of 19 patients had new ipsilateral lesions on the diffusion-weighted images after stent implantation in the carotid bifurcation, and two of these four patients had neurologic symptoms. Ohki et al (7) demonstrated that the average size of particles is 338 μm, with a range of 120 to 2100 μm during stent implantation in the carotid bifurcation. Important intracerebral arteries as small as 100 μm in diameter may be present. However, most of the cerebral emboli and lesions depicted on diffusion-weighted MR images do not seem to cause a clinical effect and remain clinically silent.

We could not identify any statistically significant factors from the patient demographic data, characteristics of the stenoses, or procedural details that would allow differentiation between patients or procedures with negative diffusion-weighted imaging results and those with positive diffusion-weighted imaging results. Chastain et al (24) demonstrated that age has a negative effect on the rate of complications. Mathur et al (25) showed that long or multiple stenoses are independent predictors of procedural stroke. Ohki et al (7) demonstrated in their ex vivo model that an echolucent plaque and a stenosis grade of more than 90% are associated with a high number of embolic particles. In the future, the examination of a larger patient population and the analysis of more factors (especially plaque morphologic features) may allow identification of subgroups of patients who have a high rate of positive findings on postprocedural diffusion-weighted images.

Müller et al (19) detected ipsilateral lesions on diffusion-weighted images obtained in 26 (34%) of 77 patients after carotid endarterectomy. Only five of these 26 patients with positive diffusion-weighted imaging results were symptomatic during or after the procedure. Compared with the other procedures, the procedures that caused positive diffusion-weighted imaging results were associated with a higher total microembolic count, as determined with transcranial Doppler monitoring during the operation. These data demonstrate that, after any manipulation of the carotid artery, new postprocedural lesions can occur in as many as one third of patients, an most of them are asymptomatic.

Despite the uncertainty regarding the prognostic value of signal intensity abnormalities on diffusion-weighted images, the presence of fewer emboli and, consequently, fewer lesions on diffusion-weighted images should be assumed to be beneficial to the patient. In this context, diffusion-weighted imaging can be used as a quality assessment tool. It allows comparison of the results of different treatment options for a high-grade stenosis in the carotid artery. Also, it can be used to identify subgroups of patients who may be at high risk for cerebral embolization and subsequent cerebral ischemia. It could help in determining the effect of cerebral protection devices, such as occlusion balloons and filters, during stent implantation on the occurrence of new lesions (26–27). We encourage the use of diffusion-weighted MR imaging in trials before and after stent implantation in the carotid artery to depict new areas of cerebral ischemia after the procedure.

Conclusion

Stent implantation in the carotid artery was associated with new areas of cerebral ischemia, as depicted on diffusion-weighted MR images, in 29% of all procedures. This finding indicated the occurrence of cerebral microemboli during such procedures. In all patients except one, the new lesions were clinically silent.

Acknowledgment

References

1. Mathias K, Jäger H, Hennigs S. **Technique of stent angioplasty in atherosclerotic disease of the internal carotid artery.** *Carotid Intervent* 1999;1:41–46
2. Wholey MH, Wholey MH, Jarmolowski CR, Eles G, Levy D, Buecthel J. **Endovascular stents for carotid artery occlusive disease.** *J Endovasc Surg* 1997;4:328–338
3. Yadav JS, Roubin GS, Iyer S et al. **Elective stenting of the extracranial carotid arteries.** *Circulation* 1997;95:376–381
4. Diethrich EB, Ndiaye M, Reid DB. **Stenting in the carotid artery: initial experience in 110 patients.** *J Endovasc Surg* 1996;3:42–62
5. Wholey MH, Wholey M, Bergeron P et al. **Current global status of carotid artery stent placement.** *Cathet Cardiovasc Diagn* 2000;50:160–167
6. Jordan WD Jr, Voellinger DC, Doblar DD, Plyushcheva NP, Fisher WS, McDowell HA. **Microemboli detected by transcranial Doppler monitoring in patients during carotid angioplasty versus carotid endarterectomy.** *Cardiovasc Surg* 1999;7:33–38
7. Ohki T, Marin ML, Lyon RT. **Ex vivo human carotid artery bifurcation stenting: correlation of lesion characteristics with embolic potential.** *J Vasc Surg* 1998;27:463–471
8. Manninen HI, Räsänen HT, Vanninen RL, Vainio P, Hippeläinen M, Kosma V. **Stent placement versus percutaneous transluminal angioplasty of human carotid arteries in cadavers in situ: distal embolization and findings at intravascular US, MR imaging, and histopathologic analysis.** *Radiology* 1999;212:483–492
9. Beauchamp NJ Jr, Barker PB, Wang PY, vanZijl PCM. **Imaging of acute cerebral ischemia.** *Radiology* 1999;212:307–324
10. Beauchamp NJ, Ulug AM, Passe TJ, van Zijl, PCM. **MR diffusion imaging in stroke: review and controversies.** *Radiographics* 1998;18:1269–1283
11. Burdette JH, Elster AD, Ricci PE. **Acute cerebral infarction: quantification of spin-density and T2 shine-through phenomena on diffusion-weighted MR images.** *Radiology* 1999;212:333–339
12. Burdette JH, Ricci PE, Petitti N, Elster AD. **Cerebral infarction: time course of signal intensity changes on diffusion-weighted MR images.** *AJR Am J Roentgenol* 1998;171:791–795
13. Kidwell CS, Alger JR, Di Salle F et al. **Diffusion MRI in patients with transient ischemic attacks.** *Stroke* 1999;30:1174–1180
14. Van Everdingen KJ, van der Grond J, Kapelle LJ, Ramos LMP, Mali WPTM. **Diffusion-weighted magnetic resonance imaging in acute stroke.** *Stroke* 1998;29:1783–1790
15. Lövblad K, Laubach H, Baird AE et al. **Clinical experience with diffusion-weighted MR in patients with acute stroke.** *AJNR Am J Neuroradiol* 1998;19:1061–1066
16. Bendszus M, Koltzenburg M, Burger R, Warmuth-Metz M, Hofmann E, Solymosi L. **Silent embolism in diagnostic cerebral angiography and neurointerventional procedures: a prospective study.** *Lancet* 1999;354:1594–1597
17. Britt PM, Heiserman JE, Snider RM, Shill HA, Bird CR, Wallace RC. **Incidence of postangiographic abnormalities revealed by diffusion-weighted MR imaging.** *AJNR Am J Neuroradiol* 2000;21:55–59
18. Lövblad KO, Plüschke W, Remonda L et al. **Diffusion-weighted MRI for monitoring neurovascular interventions.** *Neuroradiology* 2000;42:134–138
19. Müller M, Reiche W, Langenscheidt P, Haßfeld J, Hagen T. **Ischemia after carotid endarterectomy: comparison between transcranial Doppler sonography and diffusion-weighted MR imaging.** *AJNR Am J Neuroradiol* 2000;21:47–54
20. Fox AJ. **How to measure carotid stenosis.** *Radiology* 1993;186:316–318
21. Freeman GH, Halton JH. **Note on an exact treatment of contingency, goodness of fit and other problems of significance.** *Biometrika* 1951;38:141–149
22. Wilcoxon F. **Individual comparisons of ranking methods.** *Biometrics* 1945;1:80–83
23. Heiserman JE. **Silent embolism after cerebral angiography.** *Lancet* 1999;354:1577–1578
24. Chastain II HD, Gomez CR, Iyer S et al. **Influence of age upon complications of carotid artery stenting.** *J Endovasc Surg* 1999;6:217–222
25. Mathur A, Roubin GS, Iyer SS. **Predictors of stroke complicating carotid artery stenting.** *Circulation* 1998;97:1239–1245
26. Theron JG, Payelle GG, Coskun O et al. **Carotid artery stenosis: treatment with protected balloon angioplasty and stent placement.** *Radiology* 1996;201:627–636
27. Ohki T, Roubin GS, Veith FJ, Iyer SS, Brady E. **Efficacy of a filter device in the prevention of embolic events during carotid angioplasty and stenting: an ex vivo analysis.** *J Vasc Surg* 1999;30:1034–1044